Int J Adv Manuf Technol (2012) 61:195–204
DOI 10.1007/s00170-011-3683-x

ORIGINAL ARTICLE

Investigation on overlap joining of AZ61 magnesium alloy: laser welding, adhesive bonding, and laser weld bonding

Daxin Ren · Liming Liu · Yongfei Li

Received: 19 May 2011 / Accepted: 3 October 2011 / Published online: 18 October 2011

Abstract This paper presents the research on weldability of magnesium alloy AZ61 sheets by overlap laser welding, adhesive bonding, and laser seam weld bonding processes. Microstructures and mechanical properties of the joints are investigated. In overlap laser welding, the joint fractures at the interface between the sheets and maximum shear strength can reach 85% of that of the base metal. Off-center moment during tensile shear test can lead to the strength loss, while the weld edge can also influence the strength as a cracking source. Adhesive bonded joint can offer high tensile shear failure force but low peel strength. Laser weld bonded joint offers higher tensile shear failure force than either laser welded joint or adhesive bonded joint does, and the improved failure load is due to combined contribution of the weld seam and the adhesive. The weld seam can block the adhesive crack propagation, and the adhesive improves the stress distribution, so they can offer a synergistic effect.

Keywords Magnesium alloys · Overlap laser welding · Adhesive bonding · Laser weld bonding

1 Introduction

Magnesium and its alloys are considered as promising basic materials because of the specific characteristics, such as high strength-to-weight ratio, heat conductivity, and recyclability [1]. Interest on Mg alloys increases due to the demand for lightweight materials in aerospace and automobile applications. Therefore, a Canada–China–USA collaborative project on Magnesium Front End Research and Development has been started to increase the applications of magnesium [2].

Many welding technologies have been reported to join magnesium alloys, and satisfying welded joints were obtained. Friction stir welding technology was used to weld Mg alloys [3, 4], and Chi et al. investigated the weldability and fracture modes of AZ series Mg alloys by electron beam welding [5]. Some hybrid welding technologies were also used to weld Mg alloys. Low-power laser/arc hybrid welding could offer better welding efficiency than that of laser welding or TIG welding [6]. Active flux welding of Mg alloys was investigated, and deep penetrations were obtained with the added active flux [7]. Besides, welding of Mg and other alloys is also researched: for example, Mg alloys and copper alloys were diffusion bonded [8], and laser-arc hybrid welding was used to weld Mg and steel with interlayer [9]. Laser welding has many benefits for welding Mg alloys because of the low heat input, small heat-affected zone (HAZ), deep and narrow fusion zone (FZ), low residual stress, and high welding speed. AZ series magnesium alloys are commonly used, and the weldability by laser beam has been widely researched: CO_2 laser beam was used to weld dissimilar magnesium-based alloys by Quan et al. [10], while Nd:YAG laser was used to weld AZ91 magnesium alloy for aerospace industries by Abderrazak et al. [11]. However, butt welding is mainly reported in these papers. In many conditions, overlap welded joints are widely used especially in the auto industries, but only a few mechanical properties of overlap welding Mg alloys are reported.

Adhesive bonding has been used to join a die cast magnesium automotive door [12], and the corrosion

D. Ren · L. Liu (✉) · Y. Li
Key Laboratory of Liaoning Advanced Welding and Joining Technology, School of Materials Science and Engineering, Dalian University of Technology, Dalian 116024, People's Republic of China
e-mail: liulm@dlut.edu.cn

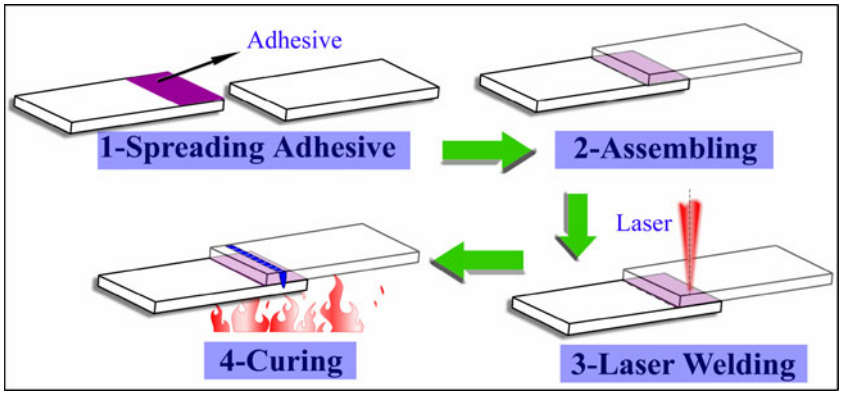

Fig. 1 Schematic diagram of laser seam weld bonding

protection was also investigated. However, adhesive also has some shortcomings, including low peel strength under out-of-plane loads, limited tolerance of low, short shelf life, short working life, and tendency of fumes [13]. Laser welding and adhesive bonding both have many benefits, but some defects are still generated to influence the strengths when joining magnesium alloys.

Weld bonding is a hybrid joining technology which combines welding with adhesive bonding. The advantages of this technology include reduced manufacturing costs, adaptability to mechanization, high static strength, improved fatigue strength, improved corrosion resistance, and the elimination of sealing operations [14]. Darwish investigated the stresses of weld bonded joint [15], reporting that the adhesive layer could strengthen and balance the stresses. Laser weld bonding of AA5754 Al alloy for automobile structures was investigated [16], and the mechanical performances were measured using shear test, peel test, and fatigue test. In the papers mentioned above, only spot welding is analyzed, and laser seam welding has not been well used in weld bonding. The schematic of laser seam weld bonding is shown in Fig. 1.

Laser welding, adhesive bonding, and laser weld bonding technologies all can be used to overlap join materials and are applied to joining AZ61 Mg alloy in recent works. The microstructures are observed, and the mechanical properties are tested. The factors that could influence the mechanical properties of the laser welded joints are discussed. Based on the influence factors, adhesive bonding and laser weld bonding are carried out to increase the joint strength, and the advantages and shortages of the three technologies are compared and discussed.

Table 1 Chemical composition and mechanical properties of AZ61 Mg alloy

Composition (wt.%)					Mechanical Properties (MPa)	
Al	Zn	Mn	Si	Mg	Tensile strength	Shear strength
6.442	0.705	0.248	0.04	Bal.	290	140

2 Experiment

AZ61 Mg alloy sheets (thickness of 1.5 mm) are used in the experiments with the chemical compositions and mechanical properties shown in Table 1. The surfaces of the Mg sheets are all cleaned with scratched brush and acetone to maintain consistent surface condition before joining.

The welding equipment is a 1-kW pulsed Nd:YAG laser welding machine. The pulsed laser with a wavelength of 1.064 μm is focused through a lens with a focal length of 150 mm, and the focus diameter on the surface of the sheet is about 0.5 mm. The main welding parameters are shown as follows: the power of the laser beam: P=600 W; 5 ms pulse duration; the pulse frequency, 40 Hz; the defocus distance, f_d=−1.0 mm; and the flow rate of 15 L/min Argon shielding gas. After welding, the cross sections of the joints are prepared by standard polishing techniques and then etched in picric acid-based etchant (acetic acid 5 ml+picric acid 5 g+ethanol 100 ml+distilled water 10 ml). The microstructures and the fracture morphology are observed by optical microscope and scanning electron microscope. A heat-curing structural adhesive Henkel 5087–02, produced by Hankel Lnc. and supplied by GM, is used for adhesive bonding, and the physical properties of the adhesive are shown in Table 2.

The thickness of the adhesive spread on the lower sheet surface is 0.08–0.1 mm. The specimens are cured in 30 min at 180°C, with a ramp up from room temperature at no more than 5°C/min. Tensile shear tests and T-peel tests are

Table 2 Properties of Henkel 5087 adhesive

	Lap shear strength	T-Peel strength	Impact peel strength
Henkel 5087-02	20.2 MPa	8.0 N/mm	33.4 MPa

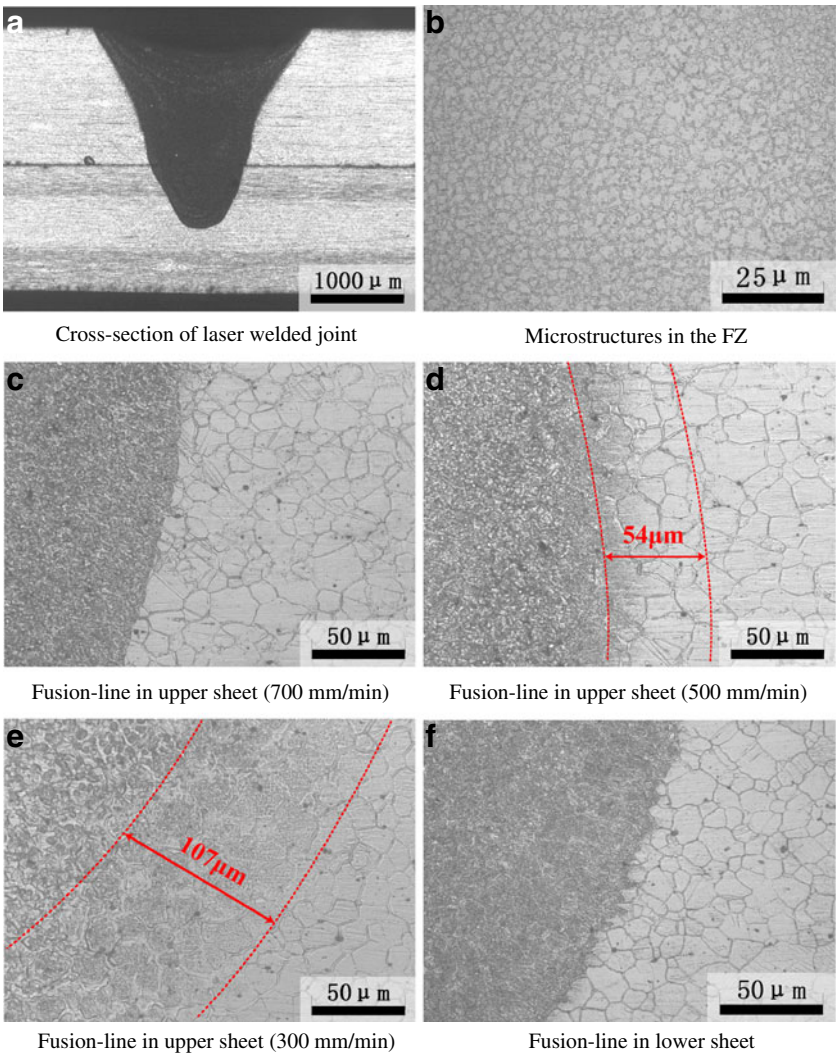

Fig. 2 Microstructures of laser welding

carried out for three joining methods, including overlap laser welding, adhesive bonding, and laser weld bonding. Each data point represents an average of at least three specimens, which are tensioned to fracture in an electronic

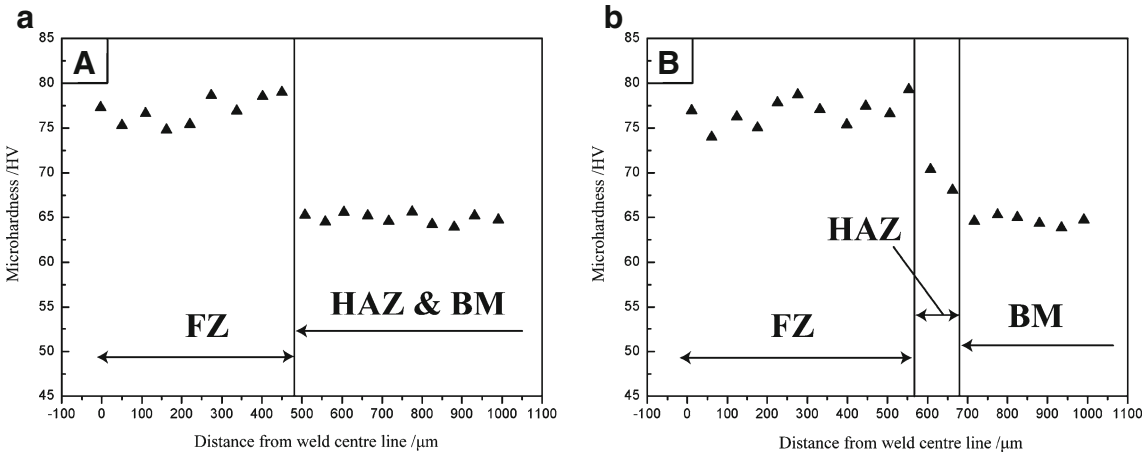

Fig. 3 Microhardness profiles of the welded joints

Fig. 4 Defects of laser welding

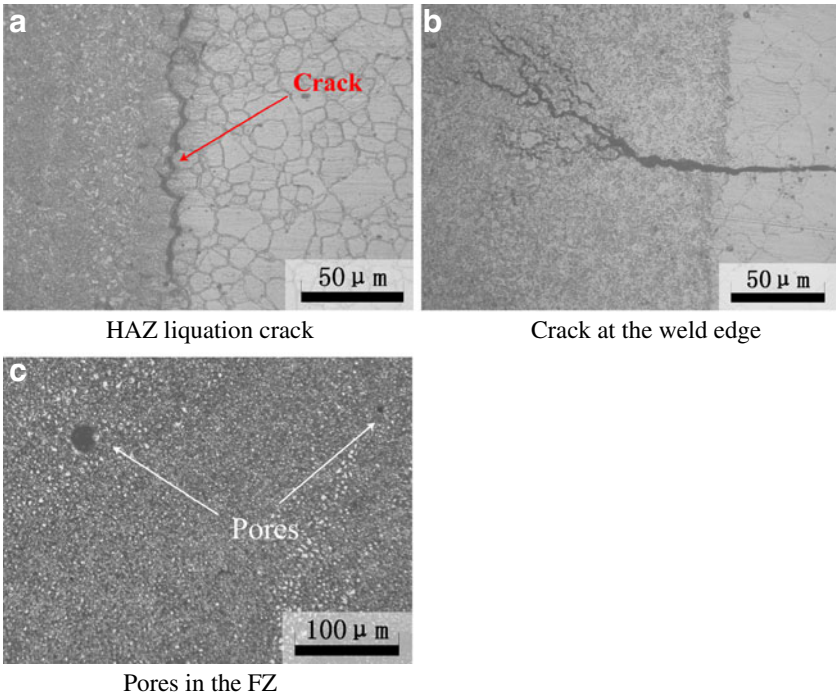

HAZ liquation crack

Crack at the weld edge

Pores in the FZ

tension machine. The cross-head velocity is 5 mm/min in order to balance the three joining methods.

3 Results and discussion

3.1 Laser welding

Figure 2 shows the cross section and microstructures of the laser welded joints. A penetration of at least 0.5 mm in the lower sheet is obtained, so that the weld width is large enough for the joint strength. Surface underfill of the weld is often obtained after welding, as shown in Fig. 2a. Strong tendency to surface underfill is due to the evaporation and ejection loss. The surface underfill could cause stress concentration to affect the joint strength. As reported, the stress concentration could lead to at least 13% strength loss in butt welding of Mg alloys [17].

Figure 2b shows the microstructures in the FZ, and the grain sizes are from 3 to 10 μm. It is seen that the grains in the FZ are refined significantly compared with that of the base metal (see Fig. 2c) due to the rapid cooling rate during laser welding. The microstructures at the fusion line in the

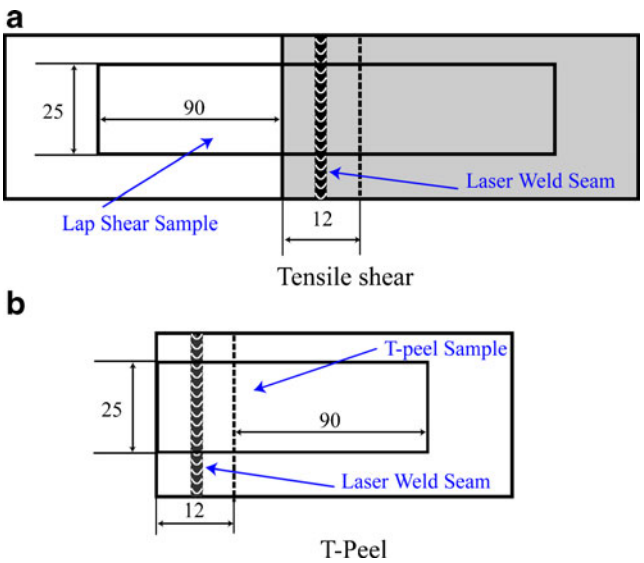

Fig. 5 Schematic specimens of laser welding

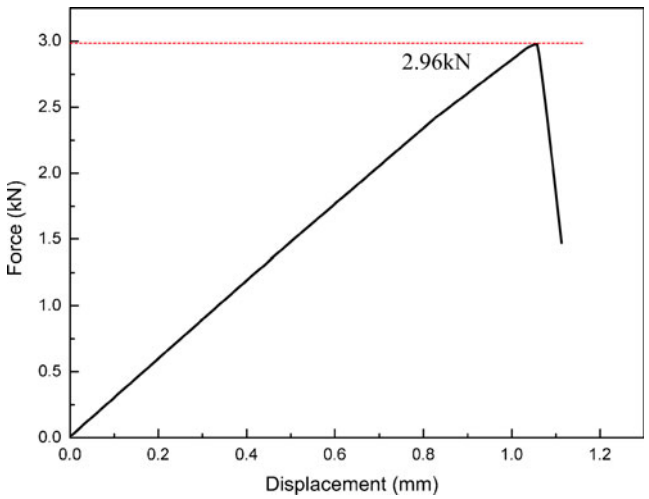

Fig. 6 Force-displacement curve of laser welded joint in tensile shear test

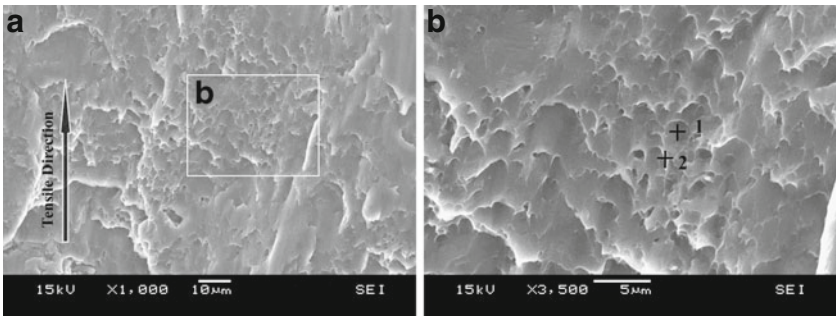

Fig. 7 Fracture morphology of the overlap laser welded joint

Dimples and cleavage planes Dimples

upper sheet are shown from Fig. 2c to e, with the welding speed of 700, 500, and 300 mm/min. The widths of HAZ are 10–110 μm, several grains wide, depending on welding speed or laser power. The width of HAZ increases as the welding speed decreases with the same laser power. When the welding speed is 700 mm/min, only very narrow HAZ can be observed (see Fig. 2c). As the welding speed decreases to 500 mm/min, no distinct grain growth occurs, but a partially melted zone of about three grains wide is observed with the liquation of the grain boundaries (see Fig. 2d). When at a low welding speed of 300 mm/min, liquation of the grain boundaries and precipitated phases increase, and the HAZ width is about 107 μm. Figure 2f shows the microstructures at the fusion line in the lower sheet. No distinct HAZ can be observed, because the cooling rate of the FZ in the lower sheet is higher than that in the upper sheet. From the microstructures, it can be concluded that the HAZ width depends on the heat input, and increased heat input would result in larger HAZ width.

Hardness distribution in the middle of weld in the upper sheet is presented in Fig. 3. It can be seen that the hardness profile shows a gradual increase in hardness from the base metal value, through the heat-affected zone, to the peak in hardness in the fusion zone. When the welding speed is 700 mm/min, the hardness shows a sharp decrease from the FZ to the base metal (BM), illustrating that the HAZ is very narrow. When the welding speed decreases to 300 mm/min, a hardness transition zone can be seen between the FZ and BM, and the width is almost equal to that of the partially melted zone. The increased hardness of the fusion zone and the partially melted zone is due to grain refinement and precipitation.

Table 3 Chemical compositions of the points on the fracture surface

	Composition (wt.%)			
	Mg	Al	Zn	Mn
P1	92.74	6.32	0.69	0.25
P2	92.34	6.73	0.68	0.25

Some HAZ liquation cracks can be observed at a low welding speed as shown in Fig. 4a. During the welding thermal cycles, the phases with low melting point would melt. As the alloying elements and impurities segregate at the grain boundaries, the HAZ becomes brittle. Similar results are also reported by Cao et al. [18], and the partially melted zone is often obtained in welding Mg alloys with high content of Al and Zn. Under the stresses induced by the thermal cycles, cracking of the brittle grain boundaries occurs, even sometimes extending from HAZ to FZ. Cracks can sometimes be observed at the FZ edge between the sheets, as shown in Fig. 4b. In overlap laser welding, the FZ edge is the position with high stress concentration during rapid cooling, because it is between the BM of low temperature and FZ of high temperature. The temperature gradient leads to different expansions between BM and FZ, and the stress may lead to the cracks. Especially during pulse laser welding, molten pool may melt and solidify periodically depending on the laser pulse overlapping factor, so the trend of cracking may increase. In addition, the welding deformation and the clamping devices can also influence the crack [18].

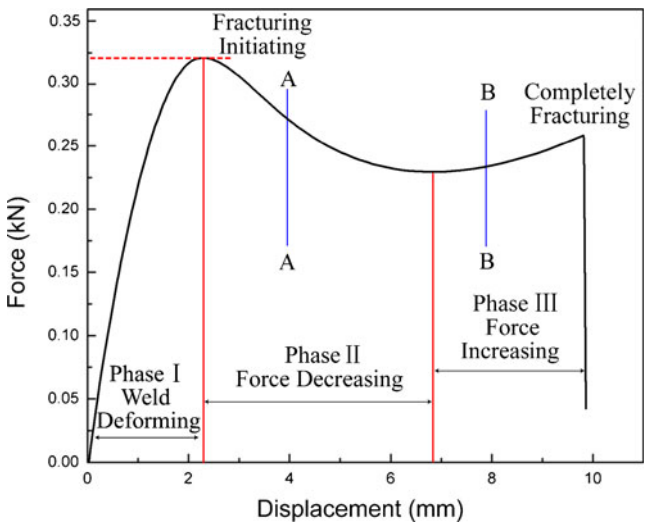

Fig. 8 Force-displacement curve of T-peel tests of laser welded joints

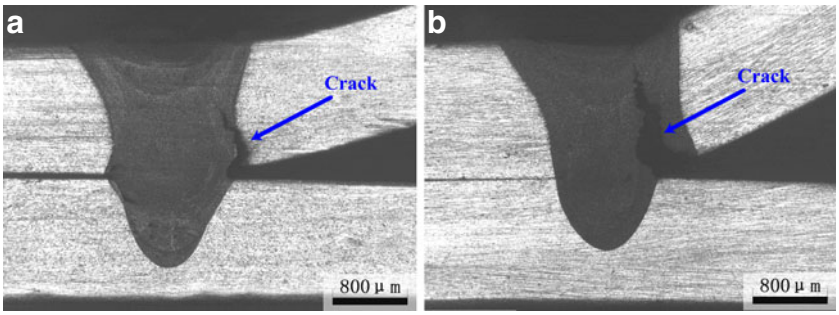

Fig. 9 Cross sections of joints in T-peel test

Cross-section at position A-A Cross-section at position B-B

Cavity defects in the FZ can be observed in the joint as shown in Fig. 4c. It is expected that the collapse of instable keyholes may cause pores under the condition of pulsed laser and overlapped sheets in this experiment. Magnesium alloys have stable laser keyholes due to the high equilibrium vapor pressure, low boiling temperature, and low surface tension, but the gap between the sheets can make the instability of the keyhole to increase. Therefore, some pores are formed after solidification of the FZ.

Mechanical properties of the laser welded joints are measured. The schematic specimens of laser welding are shown in Fig. 5, and the tensile shear result is shown in Fig. 6. An interfacial fracture occurs between the sheets, and the tensile shear strength of the joint is about 120 MPa, 85% of that of the base metal (140 MPa).

HAZ is not the factor leading to the strength loss, because a fracture does not occur at the FZ–HAZ interfaces. Some defects and the overlap structure may result in the strength loss. Firstly, magnesium alloys have notch sensibility, and the weld edge between the sheets may lead to fracture as a potential cracking source in overlap welding, especially when solidification cracks exist. Secondly, stress concentration can influence the strength significantly. Thirdly, existence of the off-center moment during tensile shear test can reduce the strength. In tensile shear test, the overlap laser welded joint can deform, so the peel stress at the weld edge can deteriorate the strength.

Fracture morphology of the overlap laser welded joint is shown in Fig. 7, which is different from those of butt laser welded joint as reported. Some dimples can be found on the fracture surface, while large cleavage planes can also be observed. The fracture surface shows mixed fracture with both ductile deformation and brittle deformation during the tensile shear test. Mg alloys have limited deformability at room temperature due to the hexagonal close-packed crystal structure, so the fracture surface shows some cleavage planes. The dimples at local regions are caused by fracturing of the elongated grains along the tensile direction during the test. The dimples on the fracture surface are shallow, and the sizes are very small with diameters only from 3 to 5 μm. As shown in Fig. 2b, the grains refine significantly due to the high cooling rate, and the smallest sizes of the grains are about 3 μm, which are approximately equal to that of the dimples. The refined grains of the weld can lead to better deformability, so the dimples can be generated at the region where the very small grains existed. The EDS results indicate that Al content in the dimple is slightly lower than that at the dimple boundary as shown in Table 3. After solidification, the alloying elements, such as Al and Zn, can segregate at the grain boundaries, so the dimple boundary shows higher alloying contents after transcrystalline fracture occurs.

The welded joint fractures in the weld seam in the upper sheet after T-peel test in Fig. 8 show the force-displacement

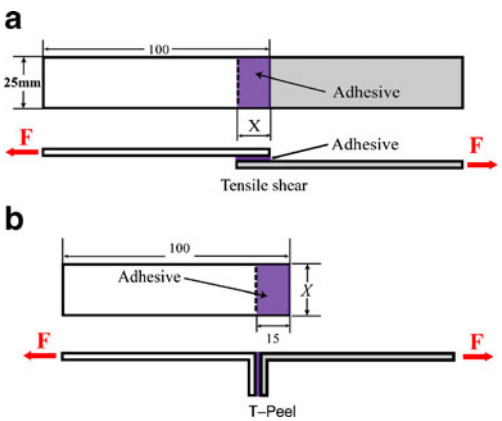

Fig. 10 Schematic specimens of adhesive bonding

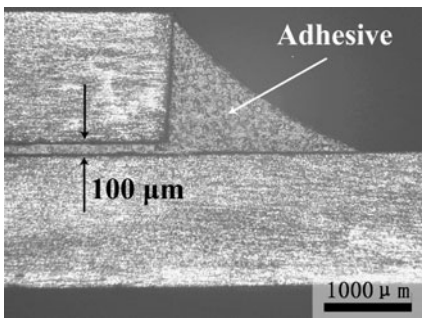

Fig. 11 Cross section of adhesive bonding

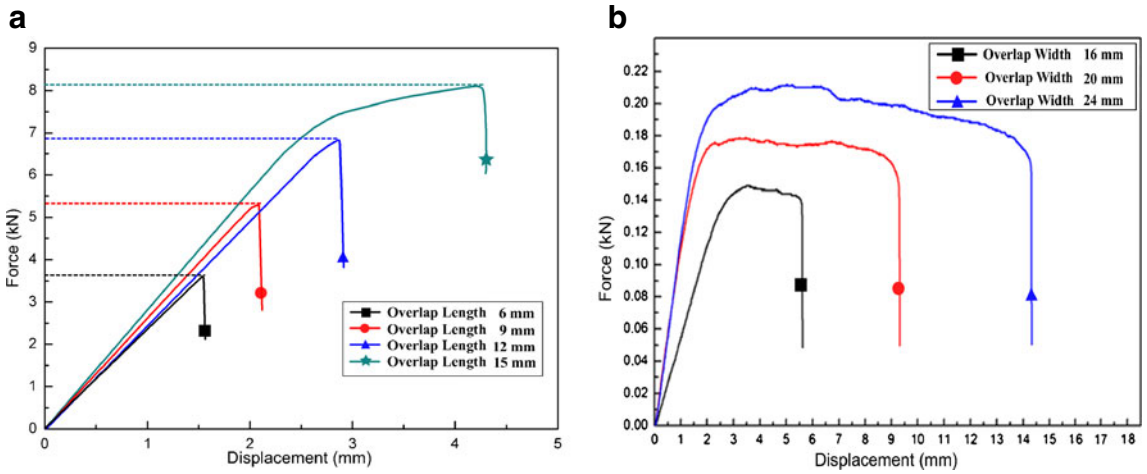

Tensile shear results T-peel results

Fig. 12 Test results of adhesive bonding

curve. The curve indicates three distinguishing phases (phase I, II, and III) during the peel test. In phase I, the force increases sharply as the weld begins to deform, and maximum 0.32 kN can be obtained at the curve top. In the next phase, the force decreases non-linearly at a lower rate as the displacement increases. Finally, the force increases again until the specimen completely fractures in the last phase. Cross sections of the joints during T-peel tests are prepared to investigate the fracture characteristics. In the following T-peel test, the force is unloaded as the curve begins to decrease at the approximate position of A–A in Fig. 8, and then the cross section of weld is observed as shown in Fig. 9a. By the same method, when the curve begins to increase at the position of B–B, the cross section is prepared as shown in Fig. 9b.

Figure 9a indicates that after the sheet initially deforms and the force reaches maximum, the joint begins to fracture from the FZ edge towards the center. After laser welding, average microhardness in the FZ (81 HV) is higher than that of the BM (72 HV) due to the grain refinement and precipitation. Besides, magnesium has notch sensibility and low deformability at room temperature, so the crack extends rapidly and the force begins to decrease. After this phase, the fracturing process becomes stable, and crack continues to extend as shown in Fig. 9b, so the force increases until the specimen completely fractures.

3.2 Adhesive bonding

Tensile shear and T-peel tests are set to investigate adhesive bonding mechanical property as shown in Fig. 10. In tensile shear test, different overlap lengths are applied. While in T-peel test, different overlap widths are carried out. The etched cross section of the bonded joint is shown in Fig. 11, and the curves of force displacement are shown in Fig. 12.

The tensile shear results depend on the overlap length. When the overlap widths are all 25 mm, the forces enhance as the overlap length increases, and the shear strength is about 21 MPa. T-peel force depends on the overlap width, and the average peel strength is about 8 N/mm.

3.3 Laser weld bonding

In sum, some problems exist in overlap laser welding (LW) and adhesive bonding (AB) of AZ61 Mg alloy. The result

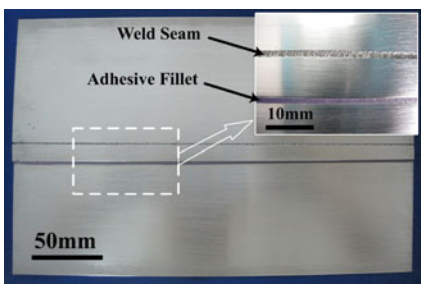

Fig. 13 Specimen of laser weld bonding

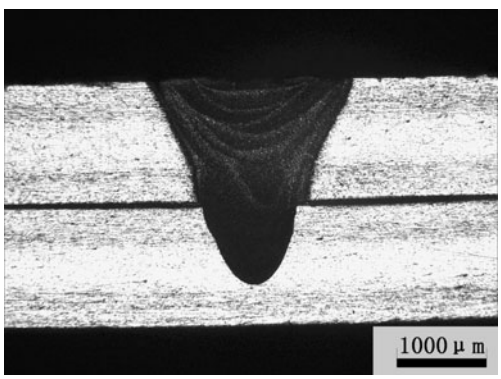

Fig. 14 Cross sections of laser weld bonded joint

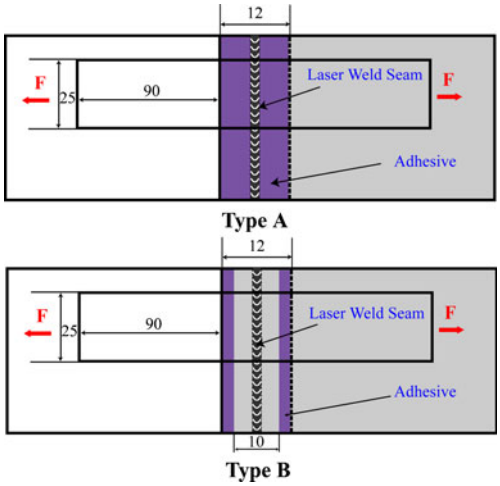

Fig. 15 Schematic specimens of laser weld bonding

shows that the maximum failure force of laser welded joint can only reach about 30% of that of the base metal. Fusion zone of laser welding is characterized by high depth-to-width ratio, and the weld width is commonly narrow. The shear strength of AZ61 Mg alloy is 140 MPa, so high shear failure force cannot be obtained by overlap laser welded joint with narrow weld width. Besides, if the weld width is increased by decreasing speed or increasing laser power, high heat input could lead to greater surface underfill to worsen the strength. It would be an ideal structure if the welded joint could offer as high a failure force as that of the base metal in the industry, so the failure force should be increased to meet the requirement. Adhesive bonding can offer high tensile force due to large bonded area, but the peel strength is low under out-of-plane loads. Adhesive bonding also has some other shortcomings, such as limited tolerance of low or even moderately high temperatures and short working life, so its application is limited to some

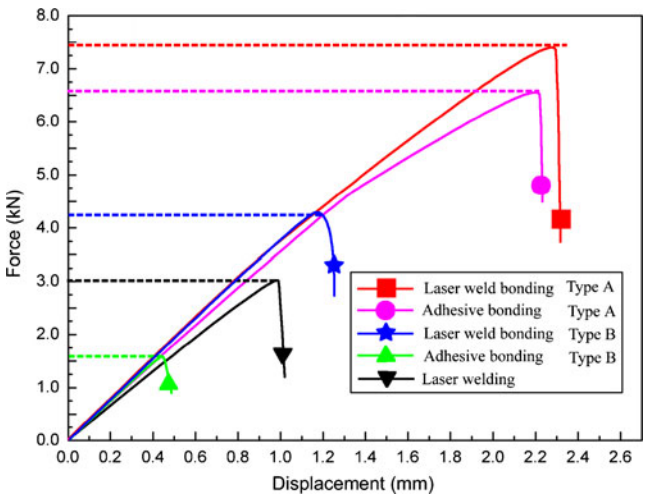

Fig. 16 Tensile shear results of the laser weld bonding, adhesive bonding, and laser welding

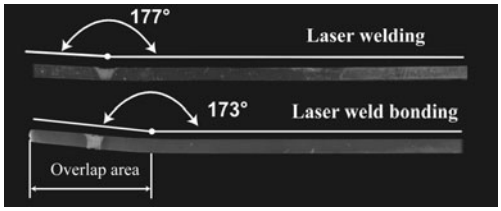

Fig. 17 Deformation angles of the fractured joints

extent. Therefore, laser weld bonding (LWB) is applied to joining Mg AZ61 alloy to increase the failure force.

The LWB specimen is shown in Fig. 13, and the cross section of LWB joint is shown in Fig. 14. The weld seam and the microstructures of LWB joints are the same as those of the LW joint, so they are not discussed in this section.

Two types of LWB joints are carried out in the tensile shear test to discuss the mechanical property comparison, and the schematic specimens are shown in Fig. 15. In type A, a large part of adhesive is set to obtain high bonding force. In type B, lengths of the adhesive bonded part at the free ends are only 1 mm in order to investigate the influence of adhesive on the mechanical property.

Figure 16 presents the tensile shear result comparison of the laser weld bonding, adhesive bonding, and laser welding. The results indicate that LWB joints offer higher failure force than either AB joints or LW joint does. The increased failure force is due to the combined contribution of adhesive bonding and laser welding.

In the test of type A, adhesive bonding offers the dominating force, and difference between failure loads of LWB joint and AB joint is 0.7 kN. The laser weld seam can offer an “anchoring” effect to increase the failure force. The fused metal of the upper sheet and lower sheet can block the adhesive crack propagation along the adherend–adhesive interfaces. Therefore, the LWB joint can offer higher failure force than the AB joint.

In the test of type B, the small adhesive bonded part can only offer 1.6 kN failure force, but the LWB joint can offer 4.2 kN failure force, and the weld seam fractures at the interface between the sheets. The failure force of the LWB joint is also higher than that of the LW joint of 3.0 kN, so it can be seen that small adhesive bonding force also can lead to the increase of failure force. Besides, the synergistic effect is better than that in type A. In this type, the weld seam offers the dominating force, and adhesive can offer the assistant influence. The adhesive can spread the force around the laser weld to soften stress concentrations, so the

Table 4 Maximum peel force comparison

	Laser welding	Adhesive bonding	Laser weld bonding
Maximum peel force/N	320	210	327

stress at the weld edge can be reduced. As discussed above, the off-center moment and stress concentration can influence the overlap laser welded joint, and the sheet deformation exists obviously during tensile shear test. The deformation angles of the upper sheet are measured after the joint fracturing, and the longitudinal sections are shown in Fig. 17.

From Fig. 17, it can be seen that the deformation angle of the LW joint is about 3°, and the deformation occurs at weld edge. The deformation angle of the fractured LWB joint is greater than that of the LW joint due to higher failure force, and deformation position is the free end of the adhesive bonded part. In LW, the tear stress would exist at the weld edge due to off-center moment, and this would reduce the joint strength. When the adhesive is added, the tear stress can be transferred from the weld edge to the free end of the adhesive bonded part. As a result, the stress concentration distribution is improved for the laser weld seam, and the effect of off-center moment is reduced. A similar result is reported by Chang et al. [19], and they claim that the stress concentration at the periphery of the nugget can be reduced significantly by the application of adhesive. Therefore, the failure force is increased after adhesive is added. The bonding force and the welding force can synergistically interact to enhance the strength, so the LWB joints of both types can offer better mechanical property than the separate technologies.

The customary way to measure the peel strength of adhesive bonding is by average peel force, and it is common to measure that of welds by the maximum force. In laser weld bonding, the maximum force is considered, and the peel property comparison of the three joining technologies is shown in Table 4.

It can be seen that the maximum peel force of LWB specimen is expected to be equal to that obtained from a conventional laser welded joint, and they are both lager than that of adhesive bonding. Santos et al. [20] also offer similar results, showing that no significant differences in peel strength were found since the resistance to peeling is mainly set by the weld nugget. This is because during the peel test, the weld seam and adhesive bonded part cannot carry the load at the same time. Adhesive ability of carrying loads out of plane is poor compared to that of carrying loads in plane, so the maximum T-peel force of weld bonded joint can only depend on the peel resistance of laser welded joint.

Laser weld bonding offers improvements in tensile shear strength compared to both laser welding and adhesive bonding, and in T-peel strength compared to adhesive bonding. The synergistic effect between the two processes in combination can lead to the strength performance enhancement, and this can increase the mechanical properties of overlap joint of Mg AZ61 alloy.

4 Conclusion

Overlap laser welding, adhesive bonding, and laser weld bonding are successfully applied to joining Mg AZ61 sheets. Microstructures and mechanical properties of overlap joints are investigated in the present paper. From the above discussions, some conclusions can be reached as follows:

1. The maximum tensile shear strength of laser welded joint reaches 85% of that of the base metal. The joint fractures at the interface between the sheets and the fracture surface show mixed fracture morphology. The strength loss is due to the weld edge and off-center moment. In peel test, the weld seam fractures in the upper sheet. Low deformability, high microhardness, and notch sensibility can result in three phases during the peel test.
2. Adhesive bonding can offer high tensile shear failure force due to the large bonding surface area. The tensile shear strength is about 21 MPa.
3. Laser weld bonding has excellent property appearance in static tensile shear test compared to laser welding and adhesive bonding due to the synergistic effect. The weld seam can block the adhesive crack, and the adhesive can optimize the stress distribution and offer high failure force due to large bonded part. The maximum peeling strength is equal to that of the conventional laser welded joint, which is an improvement compared to adhesive bonding.

Acknowledgments The authors gratefully acknowledge the sponsorship from the National Natural Science Funds of China for Distinguished Young Scholar (51025520).

References

1. Kulekci M (2008) Magnesium and its alloys applications in automotive industry. Int J Adv Manuf Technol 39:851–865
2. Luo A, Nyberg A, Sadayappan K, Shi W (2008) Magnesium front and research and development: a Canada-China-USA collaboration. The Minerals, Metals & Materials Society: Magnesium Technology: 3–10
3. Padmanaban G, Balasubramanian V (2010) An experimental investigation on friction stir welding of AZ31B magnesium alloy. Int J Adv Manuf Technol 49:111–121
4. Yamamoto M, Gerlich A, North T, Shinozaki K (2007) Cracking in the stir zones of Mg-alloy friction stir spot welds. J Mater Sci 42:7657–7666
5. Chi C, Chao C, Liu T, Wang C (2006) A study of weldability and fracture modes in electron beam weldments of AZ series magnesium alloys. Mater Sci Eng A 435–436:672–680
6. Hao X, Song G (2009) Spectral analysis of the plasma in low-power laser/arc hybrid welding of magnesium alloy. IEEE Trans Plasma Sci 37:76–82

7. Zhang Z, Zhang F (2009) Spectral analysis of welding plasma of magnesium alloy using flux coated. Mater Trans 50:1909–1914
8. Mahendra G, Balasubramanian V, Senthilvelan T (2009) Developing diffusion bonding windows for joining AZ31B agnesium and copper alloys. Int J Adv Manuf Technol 42:689–695
9. Qi X, Song G (2010) Interfacial structure of the joints between magnesium alloy and mild steel with nickel as interlayer by hybrid laser-TIG welding. Mater Des 31:605–609
10. Quan Y, Chen Z, Gong X, Yu Z (2008) CO2 laser beam welding of dissimilar magnesium-based alloys. Mater Sci Eng A 496:45–51
11. Abderrazak K, Salem WB, Mhiri H, Bournot P, Autric M (2009) Nd:YAG laser welding of AZ91 magnesium alloy for aerospace industries. Metall Mater Trans B 48:54–61
12. Bretz T, Lazarz A, Hill J, Blanchard J (2004) Adhesive bonding and corrosion protection of a die cast magnesium automotive door. Magnesium Technology: 113–119.
13. Messler R (2002) Weld-bonding: the best or worst of two processes. Ind Robot 29:138–148
14. Darwish M, Ghanya A (2000) Critical assessment of weld-bonded technologies. J Mater Process Technol 105:221–229
15. Darwish M (2003) Weld bonding strengthens and balances the stresses in spot-welded dissimilar thickness joints. J Mater Process Technol 134:352–362
16. Messler R, Bell J, Craigue O (2003) Laser beam weld bonding of AA5754 for automobile structures. Weld J 82:151–159
17. Chi C, Chao C (2007) Characterization on electron beam welds and parameters for AZ31B-F extrusive plates. J Mater Process Technol 182:369–373
18. Cao X, Xiao M, Jahazi M, Immarigeon JP (2005) Continuous wave ND:YAG laser welding of sand-cast ZE41A-T5 magnesium alloys. Mater Manuf Process 20:987–1004
19. Chang B, Shi Y, Lu L (2001) Studies on the stress distribution and fatigue behavior of weld-bonded lap shear joints. J Mater Process Technol 108:307–313
20. Santos I, Zhang W, Goncalves V, Bay N, Martins P (2004) Weld bonding of stainless steel. Int J Mach Tool Manuf 44:1431–1439